Journal of Industrial and Management Optimization

https://www.aimspress.com/journal/jimo

JIMO, 22(10): 4770–4795
DOI:10.3934/jimo.2026165
Received: 18 April 2026
Revised: 17 August 2026
Accepted: 01 September 2026
Published: 08 September 2026

Research article

Price-induced stable matching in shared healthcare

Xiaowei Lin[1] **and Yun Wei**[2,*]

[1] Department of Fundamental Courses, Nanjing University of Industry Technology, Nanjing, Jiangsu, 210023, China

[2] Nursing Division of the Department of Cardiology, Nanjing Drum Tower Hospital Affiliated to Nanjing University Medical School, Nanjing, Jiangsu, 210008, China

* **Correspondence:** Email: weiyun@njglyy.com; Tel: +86-159-5198-6678.

Abstract: Platform-mediated home healthcare requires coordinated pricing and assignment among clinically and geographically heterogeneous patients and nurses. We develop a price-induced stable matching (PISM) model for a medical institution-affiliated platform that posts a service fee, applies a fixed nurse compensation share, and computes a stable one-to-one assignment. In the single-tier setting, price changes bilateral participation and the mutually acceptable graph without reordering within-tier preferences. On a finite admissible price grid, an optimal fee exists; under explicit local fluid conditions, the profit benchmark exceeds the volume benchmark; and platform profit is invariant across patient- and nurse-proposing stable mechanisms when margins depend only on price and service type. A tiered extension shows how compensation differences can reorder advanced nurses' cross-tier preferences and generate downward substitution. Externally anchored synthetic experiments across six supply–demand and spatial configurations yield nurse rule-conditional price-induced welfare losses of 1.47%–14.41%. Hospital-clustered nurse origins materially increase travel but change the profit-optimal fee only modestly, whereas valuation dispersion has stronger effects on price and completed volume. A two-dimensional price search reveals a nonmonotone relationship between the compensation premium and downward substitution.

Keywords: shared healthcare; two-sided matching; spatial pricing; price-induced stability; downward substitution; gig economy; operations management
Mathematics Subject Classification: 91B68, 90B80, 91B24, 90B90

1. Introduction

Population aging and the diffusion of digital health technologies are extending professional nursing services from hospitals to communities and patients' homes. In China, the Internet Plus Nursing Service

(IPNS) program is organized around a model of "online application and offline service" in which qualified medical institutions use registered nurses to serve assessed patients at home [1,2]. Related arrangements also appear internationally in home care agencies and digitally mediated professional service platforms. These systems can improve access for older adults, patients with mobility limitations, and patients requiring post-discharge care, but they also create operational questions concerning service pricing, nurse compensation, clinical compatibility, travel burden, and assignment.

Home nursing differs from standardized ride-hailing in three respects. First, an edge between a patient and a nurse must satisfy clinical, credential, time window, and risk assessment requirements before economic preferences are considered. Second, patients may value nurse-specific attributes such as professional title, experience, institutional affiliation, specialty certification, and reputation. Third, nurses affiliated with medical institutions can still retain meaningful acceptance preferences because home visits are often performed in limited time blocks and impose heterogeneous travel, safety, and opportunity costs. Recent discrete choice evidence shows that compensation, personal safety, service duration, commute time, and service type materially affect nurses' willingness to undertake Internet Plus nursing work [3,4].

1.1. Theoretical gap and motivation

From an operations perspective, platform-mediated home nursing combines pricing with a two-sided assignment problem. The home healthcare routing and scheduling literature captures time windows, skill compatibility, continuity, and travel, but commonly assumes that a centralized provider controls assignments. Spatial platform pricing models allow self-interested supply but are mainly developed for homogeneous transportation services. Matching theory and matching with contracts permit bilateral preferences and transfers, yet they do not by themselves specify how a regulated or institution-affiliated platform's posted service fee, compensation rule, clinical compatibility, and spatial frictions jointly determine the acceptable graph.

A precise distinction is important. With a common fee and a fixed nurse compensation share, a price changes whether a patient–nurse pair is mutually acceptable, but the common monetary term cancels from comparisons among alternatives within the same service tier. Hence, uniform pricing is a participation and edge-selection mechanism, not a within-tier reranking mechanism. Reranking arises in the tiered extension because advanced and basic requests generate different nurse compensation. This distinction motivates our price-induced stable matching (PISM) framework and avoids attributing preference changes to a common price when only outside option comparisons change.

1.2. Research questions and main contributions

Motivated by these operational features, we address four questions:

1. How do nurse attributes, nonlinear travel friction, and posted prices jointly determine mutually acceptable patient–nurse edges?
2. Under what conditions does an optimal platform price exist in a finite stable-matching market?
3. Do different stable selection rules change the platform's optimal price, assignments, or welfare?
4. How does tier-specific compensation reorder advanced nurses' preferences and create or limit downward substitution?

The paper makes three contributions. First, it formulates an equilibrium-constrained pricing problem with a closed payment flow: The patient pays the service fee, a fixed share compensates the nurse, and the remainder funds platform operations. Second, it establishes existence for the operational finite price grid, characterizes pairwise price feasibility intervals, and derives an invariance result across stable selection rules. The continuous fluid comparison between profit- and volume-maximizing prices is stated under explicit derivative and single-peakedness conditions rather than as a universal pricing distortion property. Third, it extends the model to skill-tiered services, where compensation differences can reorder advanced nurses' preferences. The extension distinguishes priority separation from complete market separation and identifies a capacity absorption condition that, together with priority separation, is sufficient to guarantee zero downward substitution under the maintained nurse-proposing rule.

2. Literature review

The study connects five research streams: home healthcare operations, Internet Plus nursing implementation and participant preferences, spatial platform pricing, two-sided matching and matching with contracts, and resource flexibility.

2.1. Home healthcare operations and internet plus nursing

Home healthcare routing and scheduling research jointly studies caregiver assignment, routing, time windows, continuity of care, and skill compatibility [5–7]. Recent work has expanded the scope to endogenous patient time window options, uncertain referrals and repeat visits, and more flexible formulations [8, 9]. This literature provides detailed representations of clinical and logistical feasibility. Its principal decision maker, however, is typically a centralized agency that assigns employed caregivers to routes. Our setting instead focuses on a single service block in which affiliated nurses can reject economically or operationally unattractive tasks. The resulting assignment must therefore be both clinically feasible and stable with respect to the reported preferences of patients and nurses.

The closest operational comparator is [10], which matched daily home healthcare demand with heterogeneous caregiver supply on a service-sharing platform using centralized optimization and alternative stakeholder objectives. Their formulation incorporates routing, breaks, temporal dependencies, and flexible service durations. Our study complements that work by endogenizing a common posted fee and the associated nurse compensation, treating both sides' acceptability and rankings as constraints on assignment, and requiring the resulting one-service-block matching to be stable. Thus, the distinction is not between platform and nonplatform home care but between centralized operational assignment at given economic primitives and equilibrium pricing with bilateral stability.

Research on China's IPNS program provides direct institutional and empirical motivation. National policy defines the model as medical institutions using their registered nurses to respond to online applications and deliver offline home services [1,2]. A discrete-choice experiment across hospitals in Guangdong found that income, personal safety, visit duration, medical risk protection, and training affect nurses' job choices [3]. A separate Tianjin study reported substantial heterogeneity in preferences over safety, income, family cooperation, service type, and commute time [4]. Using hospital records, [11] documented an integrated online diagnosis and home nursing workflow and showed that service type and distance are important cost determinants. These studies established that travel and nonprice attributes matter, but they do not jointly optimize posted prices and stable patient–nurse assignments.

2.2. *Patient and provider attributes in digital healthcare*

Healthcare choice involves trust and quality attributes that are less salient in homogeneous delivery markets. Patients may value provider continuity, professional qualification, institutional reputation, waiting time, communication mode, insurance coverage, and price. Discrete choice studies of Chinese online–offline follow-up services show significant heterogeneity in preferences for cost, waiting time, provider continuity, hospital level, and payment method [12,13]. These findings motivate the nurse attribute vector and heterogeneous patient coefficients in our utility specification. On the supply side, the evidence in [3] and [4] motivates heterogeneous opportunity costs, travel sensitivity, and safety-related reservation values. Relative to this empirical literature, our objective is not to re-estimate preferences but to show how such estimated primitives can enter a stable pricing-and-matching mechanism.

2.3. *Pricing in two-sided spatial platforms*

Foundational two-sided market models study cross-side network effects and the allocation of fees between participant groups [14,15]. The service platform literature subsequently analyzes self-scheduling capacity, surge pricing, and spatial supply responses [16–24]. These studies demonstrate that prices can influence participation and relocate capacity. Most spatial pricing models, however, concern relatively homogeneous service providers and do not include clinical qualification, provider-specific patient preferences, or stable selection constraints. We retain the participation logic of this literature while adding a medically constrained compatibility graph and bilateral preferences.

2.4. *Two-sided matching, contracts, and endogenous participation*

Stable matching originates with [25] and has long been applied to medical labor markets [26,27]. Matching with contracts allows wages and other contractual terms to be part of an agreement [28,29]. More recent operations research has examined search design, learning, dynamic matching, and control in two-sided platforms [30–35]. We therefore do not claim that the matching literature universally assumes economically exogenous preferences. Our narrower distinction is institutional: A common posted fee and an exogenous sharing rule simultaneously determine patient participation, nurse participation, and the mutually acceptable spatial graph, and tier-specific compensation can reorder cross-tier nurse preferences. The platform anticipates the resulting stable assignment when choosing prices.

2.5. *Resource flexibility and downward substitution*

Resource flexibility research studies systems in which a high-capability resource can serve lower-tier demand [35,36]. In centralized models, the dispatcher controls whether flexible capacity is pooled. In the present setting, an advanced nurse's ranking of advanced and basic tasks depends on tier-specific compensation, task cost, and travel time. This creates a decentralized form of downward substitution. Our contribution is to derive the associated pairwise ranking threshold and a capacity absorption condition that is sufficient for ranking separation to guarantee zero cross-tier assignments under nurse-proposing deferred acceptance.

2.6. *Research positioning*

The research gap addressed in this study does not arise from any single missing component, but from the absence of a framework that jointly represents institutionally feasible home healthcare, bilateral heterogeneous preferences, a closed patient fee–nurse compensation flow, and stable assignment under platform pricing. Existing home healthcare routing and scheduling studies have provided rich representations of clinical compatibility, time windows, continuity of care, and travel, but commonly assume that a centralized provider controls caregiver assignments. Research on home healthcare service-sharing platforms further incorporates heterogeneous requests, providers, routing, and stakeholder objectives, yet generally takes economic primitives as given and does not require assignments to be stable with respect to the preferences of both patients and nurses. Empirical studies of IPNS have documented the importance of compensation, safety, service duration, commute time, provider attributes, and patient preferences, but they do not jointly optimize posted prices and matching outcomes.

Our PISM framework complements these streams by examining how a medical institution-affiliated platform's posted fee and nurse compensation rule determine bilateral participation, the mutually acceptable clinical–spatial graph, and the resulting stable assignment. Relative to spatial service platform pricing, the model introduces clinical compatibility and nurse-specific patient preferences rather than treating providers as homogeneous. Relative to stable matching and matching with contracts, it specializes the institutional setting in which the platform posts a common service fee and applies a predetermined sharing rule instead of allowing pairwise wage negotiation. Relative to resource flexibility models, downward substitution is generated by advanced nurses' endogenous cross-tier rankings rather than imposed by a centralized dispatcher. The contribution is therefore the integration of pricing, bilateral stability, healthcare-specific compatibility, heterogeneous spatial friction, and tiered resource flexibility within one operational framework.

In particular, the closest operational comparator is the centralized home healthcare service-sharing model of [10]. Our study does not replace its detailed routing and scheduling formulation; instead, it addresses a complementary decision layer by endogenizing the posted service fee and nurse compensation, allowing both sides to reject unacceptable matches and requiring the selected one-service-block assignment to be stable. This positioning also clarifies why evidence from ride-hailing and general gig platforms provides only partial motivation: Those studies inform participation and spatial pricing mechanisms, whereas the healthcare setting additionally requires clinical feasibility, provider attributes, and institutionally governed service delivery.

3. Institutional setting and service workflow

3.1. *Institutional scope*

We study a medical institution-affiliated home nursing platform rather than an unrestricted peer-to-peer labor market. Consistent with the Chinese IPNS policy, participating nurses are registered with qualified medical institutions, and a patient request must pass identity, medical record, clinical suitability, and service risk assessment before it enters the matching pool [1,2]. A medical institution may operate the digital interface itself or cooperate with a qualified technology provider. The term *platform* therefore refers to this institution–technology operational unit, which announces the fee and compensation rule, verifies eligibility, constructs the feasible graph, and facilitates assignment, payment, tracking, and evaluation.

We retain *gig economy* as a descriptor of the work arrangement, not as a claim that participating nurses are legally or organizationally independent contractors. Nurses remain institution affiliated, but they undertake discrete home visit orders in fragmented, self-selected service blocks and receive order-contingent compensation. The model captures this task-level flexibility while preserving medical institution oversight and clinical accountability.

The platform does not allow bilateral price bargaining in the model. Before matching, it posts a patient home service fee p and a nurse compensation share $\eta \in (0, 1)$. Any separately regulated clinical service item is held fixed and lies outside the pricing decision. During request submission, patients report attribute preferences or acceptable attribute ranges; patients therefore do not browse a price-ranked list of individual nurses or negotiate with them. Before price disclosure, nurses report availability, service radius, task restrictions, and the cost and travel information needed to evaluate assignments. After the fee and compensation share are disclosed, the platform combines these reports with verified nurse profiles, task details, and the posted terms to generate the price-dependent acceptable sets and strict rankings represented by Eqs (4.2)–(4.3). Both sides can reject alternatives that are unacceptable under the disclosed terms before deferred acceptance is run. This design captures the economically relevant autonomy documented in nurse preference studies while retaining the institutional safeguards of professional home care [3,4,11].

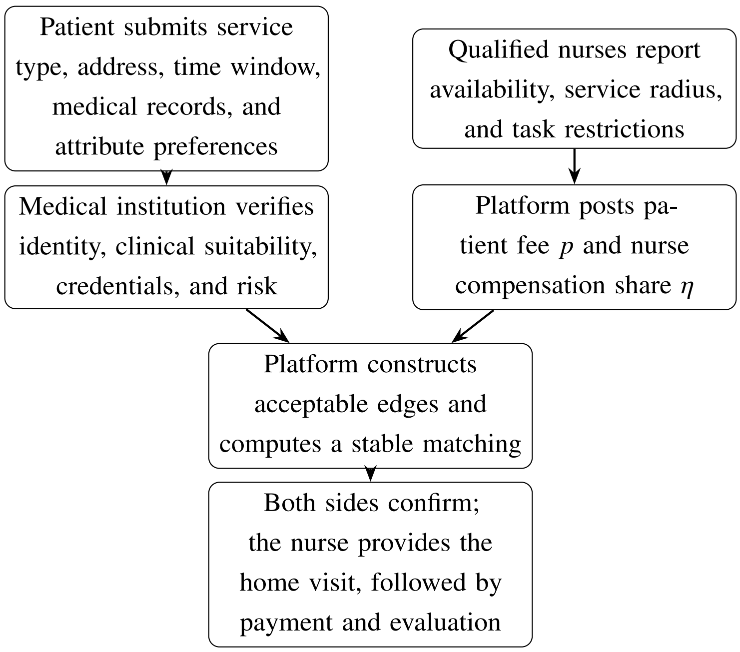

Figure 1. Operational sequence of the platform-mediated home nursing service. Matching occurs after clinical assessment, preference submission, and price disclosure and before final confirmation and service delivery.

Table 1. Main notation.

Symbol	Definition
$\mathcal{I}, \mathcal{J}; i, j$	Assessed patient and available nurse sets; representative patient and nurse
$\mathcal{P}, \mathcal{P}_\Delta; p$	Continuous institutional price envelope, operational finite price grid, and posted patient fee
η, k	Nurse compensation share and platform cost per completed transaction
$\theta_i, z_j, \boldsymbol{\beta}_i$	Patient base value, nurse attribute vector, and patient-specific attribute weights
t_{ij}, γ_i, τ_j	Door-to-door travel time, patient access sensitivity, and nurse travel cost sensitivity
$g(\cdot), h(\cdot), c_j$	Patient and nurse spatial friction functions and nurse opportunity/task cost
$a_{ij}, U_{ij}(p), \pi_{ij}(p)$	Clinical operational compatibility, patient utility, and nurse payoff
$\mathcal{E}(p), \succ_i \ (p), \succ_j \ (p); \ \succ_\mathcal{I} \ (p), \succ_\mathcal{J} (p)$	Mutually acceptable edge set, individual strict preferences, and the two preference profiles
$\mu_p^N, \mu_p^P, \mathfrak{S}(p)$	Nurse-proposing and patient-proposing outcomes and the set of stable matchings
$\mathcal{D}(p), \mathcal{N}(p); D(p), S(p)$	Active patient and nurse sets; their respective cardinalities
$Q(p, \mu_p), \Pi(p)$	Completed match quantity and finite market platform profit; $Q(p)$ is used only when the matching argument is clear or rule-irrelevant
$q(p), \bar{\Pi}(p)$	Expected matching volume and continuous fluid expected profit
$p^*, p^\Pi, p^V, p_\Phi^{SW}$	Operational grid profit optimizer, continuous fluid profit and volume optimizers, and rule-conditional operational grid welfare optimizer
$p_r^*, p_r^Q, p_r^{W,N}; W_r^N(p)$	Replication-level grid optimizers for profit, volume, and nurse-rule welfare; realized nurse-rule welfare
$L_{\text{price}}^\Phi, L_r^{N,\text{abs}}, L_r^{N,\text{rel}}$	Price-induced welfare loss under a fixed stable selection rule and its replication-level nurse-rule measures
μ^{FB}	Maximum weight clinically feasible matching used only as a stronger first best benchmark
$\mathcal{I}_H, \mathcal{I}_L, \mathcal{J}_H, \mathcal{J}_L$	Advanced/basic patient and nurse classes in the tiered extension
$p_H, p_L, \eta_H, \eta_L, \Delta w$	Tier fees, nurse shares, and advanced service compensation premium
$\boldsymbol{p}, \boldsymbol{\eta}, \mathcal{P}_2$	Tiered fee vector, share vector, and admissible two-price grid
$c_{j\ell}, k_\ell, Q_\ell$	Tier-specific nurse cost, platform cost, and completed volume

3.2. *Sequence of operations*

Figure 1 locates matching within the service chain. Matching occurs after clinical assessment, preference submission, and the announcement of fees and compensation, but before final confirmation and the home visit. Confirmation is an operational check on information already submitted. If either side declines because relevant information has changed, the platform removes that pair and reruns deferred acceptance on the updated graph; this contingency is not treated as a second equilibrium concept.

Single-period scope. The baseline model represents one service time block. Each patient requests at most one visit and each participating nurse supplies one block. This is appropriate for isolating price-induced participation and assignment effects when visits are time intensive. Repeated participation and entry or exit are introduced as a separate long-run extension in Section 5.6; they are not implicitly treated as part of the static equilibrium.

4. Model formulation

We consider one service block with a set of assessed patients $\mathcal{I} = \{1, \ldots, I\}$ and a set of available, institution-affiliated nurses $\mathcal{J} = \{1, \ldots, J\}$. The platform posts a patient fee p before matching. A fixed share $\eta \in (0, 1)$ is paid to the nurse who completes the service, and the remaining share finances platform and institutional operations. Institutional or regulatory constraints define a continuous price envelope $\mathcal{P} = [\underline{p}, \bar{p}]$. Actual posted fees use a smallest monetary adjustment unit, so the operational decision set is the nonempty finite grid

$$\mathcal{P}_\Delta = \{p_1, \ldots, p_K\} \subseteq \mathcal{P}, \qquad \underline{p} = p_1 < \cdots < p_K = \bar{p}, \tag{4.1}$$

where $\Delta = \min_{1 \le u < K}(p_{u+1} - p_u) > 0$ denotes the grid resolution. The continuous envelope remains useful for threshold characterization and the fluid comparative static benchmark.

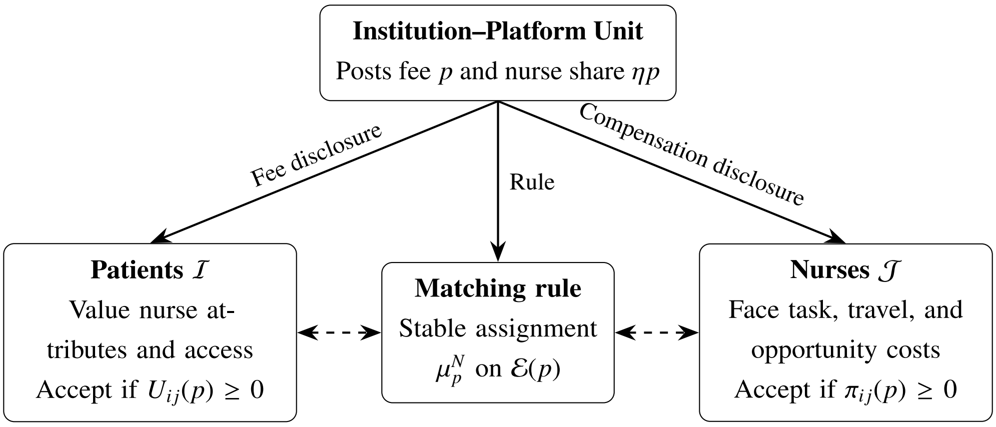

Figure 2. Payment, heterogeneous preferences, and stable matching in the baseline model.

4.1. Market primitives: Demand and supply

The baseline contains one clinically homogeneous service tier. Vertical skill differentiation is introduced in Section 6.

Patient utility (Demand side). Patient i has base value θ_i for a clinically appropriate home visit. Let z_j collect observable nurse attributes, including professional title, institutional affiliation, years of experience, specialty certification, and reputation. Patient i attaches coefficient vector $\boldsymbol{\beta}_i$ to these attributes. Let $t_{ij} \ge 0$ be the estimated door-to-door travel time from nurse j's declared origin to patient i's home. The patient's net utility is

$$U_{ij}(p) = \theta_i + \boldsymbol{\beta}_i^\top z_j - \gamma_i g(t_{ij}) - p, \tag{4.2}$$

where $\gamma_i > 0$ is patient-specific access sensitivity, and $g(\cdot)$ is increasing with $g(0) = 0$. The function can capture expected delay, punctuality risk, and geographic trust friction. Remaining unmatched yields $U_{i\emptyset} = 0$.

Nurse cost and payoff (Supply side). Nurse j has opportunity and task cost c_j and travel sensitivity $\tau_j > 0$. The nurse receives ηp after completing a service. Her net payoff from patient i is

$$\pi_{ij}(p) = \eta p - c_j - \tau_j h(t_{ij}), \tag{4.3}$$

where $h(\cdot)$ is increasing with $h(0) = 0$, and $\pi_{\emptyset j} = 0$.

Clinical and operational compatibility. Let $a_{ij} \in \{0, 1\}$ indicate whether nurse j is clinically credentialed for patient i's requested service and whether the time window, risk assessment, and geographic service boundary are compatible. Economic preferences are evaluated only when $a_{ij} = 1$. This separates medical feasibility from willingness to participate.

4.2. Nonlinear spatial friction and the linear benchmark

The main analysis requires only that g and h are continuous and increasing. The linear benchmark is nested as $g(t) = h(t) = t$. Numerical robustness can use the power family

$$g(t) = t^{\kappa}, \qquad h(t) = t^{\nu}, \tag{4.4}$$

with $\kappa, \nu > 0$, or a piecewise-linear travel cost with a higher marginal cost outside a normal service radius. Convex friction ($\kappa > 1$ or $\nu > 1$) places greater weight on long trips; concave friction weakens this localization. Heterogeneous γ_i and τ_j replace a single spatial threshold with a distribution of thresholds without changing the pairwise participation logic.

4.3. Price-induced preferences and feasibility

For $a_{ij} = 1$, patient i weakly accepts nurse j when $U_{ij}(p) \geq 0$, and nurse j weakly accepts patient i when $\pi_{ij}(p) \geq 0$. Under our weak participation convention, every compatible zero-surplus alternative is retained and ranked above remaining unmatched. A fixed, exogenous, price-independent tiebreaker orders alternatives with equal utility or payoff. Thus, the outside option is strictly below every retained edge, and the resulting preference lists are strict. Let $\succ_i (p)$ and $\succ_j (p)$ denote these strict relations. The same convention is implemented in the numerical algorithm.

We define the set of *feasible matching edges* at price p as pairs that are mutually acceptable:

$$\mathcal{E}(p) = \{(i, j) : a_{ij} = 1,\ U_{ij}(p) \geq 0,\ \pi_{ij}(p) \geq 0\}. \tag{4.5}$$

Because the common fee cancels from $U_{ij}(p) - U_{ik}(p)$, and the common nurse payment cancels from $\pi_{ij}(p) - \pi_{kj}(p)$, p does not reorder within-tier alternatives. It changes how each alternative compares with the remaining unmatched options and therefore changes $\mathcal{E}(p)$. For compactness, $\succ_{\mathcal{I}} (p) = (\succ_i (p))_{i\in\mathcal{I}}$ and $\succ_{\mathcal{J}} (p) = (\succ_j (p))_{j\in\mathcal{J}}$ denote the corresponding preference profiles.

4.4. Stable matching equilibrium

A matching is a mapping $\mu : \mathcal{I} \cup \mathcal{J} \to \mathcal{I} \cup \mathcal{J} \cup \{\emptyset\}$ such that $\mu(i) \in \mathcal{J} \cup \{\emptyset\}$, $\mu(j) \in \mathcal{I} \cup \{\emptyset\}$, and $\mu(i) = j$ if and only if $\mu(j) = i$. Stability is an assignment consistency requirement: No mutually acceptable patient–nurse pair should prefer one another to their assigned outcomes under the posted terms.

Definition 1 (Price-induced stable matching)**.** *Given a price p, a matching μ_p is stable if it satisfies:*

1. ***Individual rationality:*** *For all $i \in \mathcal{I}$ and $j \in \mathcal{J}$, if $\mu_p(i) = j$, then $(i, j) \in \mathcal{E}(p)$.*

2. ***No blocking pairs:*** *There does not exist $(i, j) \in \mathcal{E}(p)$ with $\mu_p(i) \neq j$ such that $j \succ_i (p)\mu_p(i)$, and $i \succ_j (p)\mu_p(j)$.*

For each p, the set of stable matchings $\mathfrak{S}(p)$ is nonempty. The matched sets on both sides are invariant across stable matchings in this one-to-one, strict-preference environment [27]. Individual assignments and surplus distribution can nevertheless differ.

The baseline selection rule is nurse-proposing deferred acceptance, denoted $\Phi_N(\cdot)$, because the platform uses reported nurse rankings to support voluntary acceptance. This is an algorithmic priority rule rather than a claim that nurses literally send sequential proposals in the user interface. The selected matching is

$$\mu_p^N = \Phi_N(\mathcal{I}, \mathcal{J}, \succ_{\mathcal{I}}(p), \succ_{\mathcal{J}}(p)). \tag{4.6}$$

Patient-proposing deferred acceptance and welfare-oriented selection from $\mathfrak{S}(p)$ are examined in Section 5.4.

4.5. The platform's optimization problem

Let $k \geq 0$ be the platform's per-transaction administrative, insurance, tracking, and payment-processing cost. The number of completed matches is

$$Q(p, \mu_p^N) = \sum_{i \in \mathcal{I}} \mathbf{1}\{\mu_p^N(i) \neq \emptyset\}. \tag{4.7}$$

When the matching argument is clear, we write $Q(p)$ as shorthand for $Q(p, \mu_p)$. In statements comparing stable selection rules, this shorthand is used only after rule invariance has been established. The per-match platform margin is $m(p) = (1-\eta)p-k$. The platform solves the equilibrium-constrained pricing problem

$$\max_{p \in \mathcal{P}_\Delta} \quad \Pi(p) = [(1-\eta)p - k]Q(p, \mu_p^N) \tag{4.8}$$

$$\text{s.t.} \quad \mu_p^N = \Phi_N(\mathcal{I}, \mathcal{J}, \succ_{\mathcal{I}}(p), \succ_{\mathcal{J}}(p)). \tag{4.9}$$

We use "equilibrium-constrained pricing problem" rather than the narrower mathematical programming with equilibrium constraints (MPEC) label because Eq (4.9) is an algorithmic stable matching operator, not a system of differentiable complementarity conditions.

5. Theoretical analysis

This section establishes pairwise price feasibility and operational finite-grid existence, clarifies the role of the short side of the market, compares stable selection rules, and states pricing and welfare results under explicit conditions.

5.1. Pairwise price feasibility and existence

In classical continuous demand models, demand is typically a smooth function of price. However, in finite two-sided matching markets, price variations induce discrete jumps in the topological structure of the matching network.

Define the active pools

$$\mathcal{D}(p) = \{i \in \mathcal{I} : \exists j \in \mathcal{J} \text{ with } a_{ij} = 1 \text{ and } U_{ij}(p) \geq 0\}, \tag{5.1}$$

$$\mathcal{N}(p) = \{j \in \mathcal{J} : \exists i \in \mathcal{I} \text{ with } a_{ij} = 1 \text{ and } \pi_{ij}(p) \geq 0\}, \tag{5.2}$$

and let $D(p) = |\mathcal{D}(p)|$ and $S(p) = |\mathcal{N}(p)|$.

Lemma 1 (Pairwise price-feasibility interval)**.** *For a compatible pair* (i, j)*, define*

$$A_{ij} = \theta_i + \boldsymbol{\beta}_i^{\top} \boldsymbol{z}_j - \gamma_i g(t_{ij}), \qquad B_{ij} = \frac{c_j + \tau_j h(t_{ij})}{\eta}. \tag{5.3}$$

Then, $(i, j) \in \mathcal{E}(p)$ *if and only if* $a_{ij} = 1$*, and* $B_{ij} \leq p \leq A_{ij}$*. Thus, each edge is feasible on a closed price interval, possibly empty. Patient acceptability is nonincreasing in* p*, and nurse acceptability is nondecreasing in* p*, but the mutually acceptable edge set* $\mathcal{E}(p)$ *need not be nested as* p *changes.*

We next establish existence for the operational problem. Because matching volume is threshold-driven and can be discontinuous even when the continuous price envelope is compact, compactness alone is not invoked as an existence argument.

Theorem 1 (Existence of an optimal posted fee)**.** *Suppose that* $\mathcal{I}$ *and* $\mathcal{J}$ *are finite, the operational price grid* $\mathcal{P}_\Delta$ *is finite and nonempty, weak individual rationality follows the zero-surplus convention above, and that ties are resolved by a fixed deterministic rule. Then, the platform problem* (4.8)–(4.9) *attains a global optimum* $p^* \in \mathcal{P}_\Delta$*.*

Whenever the operational grid optimizer is not unique, p^* denotes the smallest profit-maximizing price. The same smallest maximizer convention is used replication by replication in the numerical experiments.

Sketch of proof. The participation and tiebreaking conventions determine a unique selected matching and a finite profit value at every $p \in \mathcal{P}_\Delta$. The objective is therefore a real-valued function on a finite nonempty set and must attain its largest value. A full proof is in the Appendix.

Remark 1 (Continuous price benchmark)**.** *The grid assumption reflects implementable monetary increments and is also the decision domain used in the finite-market experiments. A continuous-price version over* $\mathcal{P}$ *requires an additional regularity condition, such as upper semicontinuity of the selected profit function or a specified one-sided boundary convention. The fluid analysis below uses a local continuous approximation only for comparative statics and does not substitute for the finite-grid existence result.*

5.2. The short side as an upper bound

For any price,

$$Q(p, \mu_p) \leq \min\{D(p), S(p)\}. \tag{5.4}$$

Equality is not automatic in a spatial compatibility graph: Hall-type local bottlenecks can leave active participants unmatched, even when aggregate counts are balanced. Equality may be used as a fluid approximation only under an explicit dense compatibility or asymptotic no-bottleneck condition. All finite-market computations therefore obtain Q from the matching operator rather than replacing it by $\min\{D, S\}$.

5.3. Large-market approximation and comparative statics

Although the finite grid guarantees existence for the implemented problem, extracting marginal operational insights requires a continuous state space. For this subsection only, p is allowed to vary locally in the continuous envelope $\mathcal{P}$, and we use a fluid approximation for comparative statics.

Assumption 1 (Local fluid approximation). *In a neighborhood of the price under study, the expected stable matching volume $q(p) = \mathbb{E}[Q(p, \mu_p)]$ is differentiable. This approximation smooths finite-market threshold jumps but does not impose $q(p) = \min\{D(p), S(p)\}$.*

Proposition 1 (Effect of higher nurse travel friction)**.** *Fix p, and write $\boldsymbol{\tau} = (\tau_j)_{j\in\mathcal{J}}$. If $\tau'_j \geq \tau_j$ for every nurse, then $\mathcal{E}(p; \boldsymbol{\tau}') \subseteq \mathcal{E}(p; \boldsymbol{\tau})$. Consequently, the maximum cardinality of any feasible matching is weakly lower. This edge set result does not imply that the platform's optimal price must increase: The optimal response can be upward when compensation supports supply or downward when demand attrition dominates.*

The result follows directly from Eq (4.3). The qualification concerning p^* is important: A nonmonotone optimal price path at high friction is consistent with the theory and should be treated as a numerical comparative static, not as a contradiction of a universal monotonicity theorem.

5.4. Robustness to the stable selection rule

Let μ_p^N and μ_p^P denote the nurse- and patient-optimal stable matchings. A third rule may select a minimum travel matching from $\mathfrak{S}(p)$.

Corollary 1 (Price invariance across stable rules)**.** *Under one-to-one matching and strict preferences, all stable matchings at a fixed p match the same sets of patients and nurses. If the platform margin depends only on p and the service type, then $Q(p)$, $\Pi(p)$, and the set of profit-maximizing prices are invariant across stable selection rules. Pair assignments, average travel time, patient surplus, nurse surplus, and social welfare need not be invariant.*

This corollary explains why nurse-optimal deferred acceptance is sufficient for the baseline pricing objective while also motivating numerical comparisons of distributional and welfare outcomes under alternative rules.

5.5. Platform strategies and social welfare

With the closed payment flow, the patient fee and the nurse/platform shares cancel in aggregate welfare. For any selected stable matching μ_p,

$$SW(p, \mu_p) = \sum_{(i,j)\in\mu_p} \left[\theta_i + \boldsymbol{\beta}_i^\top z_j - \gamma_i g(t_{ij}) - c_j - \tau_j h(t_{ij}) - k\right]. \tag{5.5}$$

When the continuous envelope volume maximizer set is nonempty, define

$$p^V = \min \arg\max_{p\in\mathcal{P}} q(p).$$

Thus, p^V is the smallest continuous envelope price that maximizes the expected matching volume. For any fixed stable selection rule Φ, the operational grid welfare benchmark p_Φ^{SW} is introduced below.

These are distinct benchmarks: Maximizing coverage does not generally maximize welfare because assignments differ in travel and provider quality. Proposition 2 uses p^V and p^Π for the continuous fluid volume and profit benchmarks, whereas p^* remains the operational grid profit optimizer.

Proposition 2 (Conditional pricing distortion)**.** *Suppose Assumption 1 holds,* $\arg\max_{p\in\mathcal{P}} q(p)$ *is nonempty,* $p^V < \bar{p}$*, and the continuous envelope expected profit function* $\bar{\Pi}(p) = [(1-\eta)p - k]q(p)$ *is single-peaked on* $\mathcal{P}$ *with a nonempty maximizer set. Further, assume that*

$$(1-\eta)q(p^V) + [(1-\eta)p^V - k]q'_+(p^V) > 0. \tag{5.6}$$

Then, every continuous envelope expected profit maximizer $p^\Pi \in \arg\max_{p\in\mathcal{P}} \bar{\Pi}(p)$ *satisfies* $p^\Pi > p^V$*. Without Condition* (5.6)*, the strict inequality is not guaranteed.*

Sketch of proof. The left-hand side of Eq (5.6) is the right derivative of $\bar{\Pi}(p) = [(1-\eta)p - k]q(p)$ at p^V. Positivity implies a strict local expected profit increase to the right of p^V. Global single-peakedness then rules out a maximizer at or to the left of p^V. The condition transparently balances the margin gain against first-order volume loss.

For a fixed stable selection rule Φ, let μ_p^Φ denote its selected matching, and define $p_\Phi^{SW} = \min\arg\max_{p\in\mathcal{P}_\Delta} SW(p, \mu_p^\Phi)$. Define the rule-conditional price-induced welfare loss

$$L_{\text{price}}^\Phi = SW(p_\Phi^{SW}, \mu_{p_\Phi^{SW}}^\Phi) - SW(p^*, \mu_{p^*}^\Phi). \tag{5.7}$$

This measure holds the stable selection rule fixed and compares two prices on the same operational grid. It isolates the welfare effect of the posted price choice within that mechanism. It is not the total welfare gap relative to a first best assignment and does not measure the additional effect of selecting one stable matching rather than another. A maximum-weight clinically feasible matching μ^{FB} provides the stronger first best benchmark needed for such a total-gap decomposition. This definition also replaces the incorrect interpretation of the horizontal continuous price interval $[p^V, p^\Pi]$ as a welfare area.

5.6. Long-run participation extension

The static equilibrium is conditional on the active populations in a service block. To represent entry and exit without embedding a full routing Markov decision process (MDP), let N_t^N and N_t^P be the active nurse and patient masses in period t, and let $\bar{\pi}_t$ and $\bar{U}_t$ be their expected realized surpluses. A parsimonious participation law is

$$N_{t+1}^N = (1-\delta_N)N_t^N + \lambda_N G_N(\bar{\pi}_t - f_N), \tag{5.8}$$
$$N_{t+1}^P = (1-\delta_P)N_t^P + \lambda_P G_P(\bar{U}_t - f_P), \tag{5.9}$$

where, for side $s \in \{N, P\}$, $\delta_s \in [0,1]$ is an exit rate, $\lambda_s \geq 0$ is an entry scale, $f_s \geq 0$ is an entry or request cost, and $G_s : \mathbb{R} \to \mathbb{R}_+$ is a nondecreasing response function. The index s is reserved here for market side, and r below indexes Monte Carlo replications. A long-run platform maximizes discounted profit while accounting for this fixed-point feedback. High fees can improve nurse entry through ηp but reduce patient participation; low fees have the reverse effect. The present numerical experiments remain conditional on fixed active populations and do not solve this dynamic problem. A future extension could compare the static optimum with the steady-state equilibrium after the entry, exit, and surplus response primitives have been estimated.

6. Model extensions: Skill-tiered pricing and downward substitution

Professional home nursing is vertically differentiated. Advanced nurses can perform advanced and basic services, whereas basic nurses cannot perform advanced procedures. The platform now posts patient fees $\boldsymbol{p} = (p_H, p_L)$ and uses service-specific nurse shares $\boldsymbol{\eta} = (\eta_H, \eta_L)$. Unlike a common within-tier fee, the resulting compensation difference can reorder an advanced nurse's ranking across service tiers.

6.1. Tiered market primitives and cross-tier edges

Partition patients as $\mathcal{I} = \mathcal{I}_H \cup \mathcal{I}_L$ and nurses as $\mathcal{J} = \mathcal{J}_H \cup \mathcal{J}_L$. An advanced request can be served only by $\mathcal{J}_H$, whereas a basic request can be served by either nurse type. A *downward substitution* is a realized matched pair (i, j) with $i \in \mathcal{I}_L$ and $j \in \mathcal{J}_H$. Let $c_{j\ell}$ be nurse j's task-specific opportunity and service cost for tier $\ell \in \{H, L\}$. The nurse payoff is

$$\pi_{ij}(\boldsymbol{p}) = \begin{cases} \eta_H p_H - c_{jH} - \tau_j h(t_{ij}), & i \in \mathcal{I}_H, \\ \eta_L p_L - c_{jL} - \tau_j h(t_{ij}), & i \in \mathcal{I}_L. \end{cases} \tag{6.1}$$

Patient utility follows Eq (4.2) with the relevant tier fee and tier-specific valuation. Clinical compatibility remains encoded by a_{ij}.

6.2. Cross-tier preference reordering

Let $\Delta w = \eta_H p_H - \eta_L p_L$ be the advanced service compensation premium. For $j \in \mathcal{J}_H$, a basic request i_L is preferred to an advanced request i_H if and only if

$$\tau_j[h(t_{i_H j}) - h(t_{i_L j})] > \Delta w + c_{jL} - c_{jH}. \tag{6.2}$$

Thus, downward substitution is a ranking outcome when travel cost savings from the closer basic request exceed the compensation and task cost advantage of the advanced request. With common shares, equal task costs, homogeneous τ, and $h(t) = t$, Eq (6.2) reduces to the linear distance threshold after replacing the patient fee spread by the nurse compensation spread.

6.3. Priority-separated and interleaved rankings

Definition 2 (Cross-tier ranking regimes)**.** *The market is* priority-separated *when every advanced nurse ranks every acceptable advanced request above every acceptable basic request. Otherwise, cross-tier rankings are* interleaved*. Priority separation concerns rankings; it does not remove clinically feasible cross-tier edges.*

Proposition 3 (Sufficient condition for priority separation)**.** *Fix a price vector* $\boldsymbol{p}$*. Suppose the fixed deterministic tiebreaker ranks an acceptable advanced request above an acceptable basic request whenever an advanced nurse is indifferent between them. Let*

$$\mathcal{T} = \Big\{(j, i_H, i_L) : j \in \mathcal{J}_H,\ i_H \in \mathcal{I}_H,\ i_L \in \mathcal{I}_L,\ a_{i_H j} = a_{i_L j} = 1\Big\}.$$

If $\mathcal{T} = \varnothing$*, priority separation holds vacuously. Otherwise, a sufficient condition is*

$$\Delta w \geq \max_{\substack{j \in \mathcal{J}_H,\ i_H \in \mathcal{I}_H,\ i_L \in \mathcal{I}_L \\ a_{i_H j} = a_{i_L j} = 1}} \Big\{\tau_j[h(t_{i_H j}) - h(t_{i_L j})] - (c_{jL} - c_{jH})\Big\}. \tag{6.3}$$

Under nurse-proposing deferred acceptance and priority separation, a sufficient additional condition for zero downward substitution is that the high-tier-only submarket match every advanced nurse who would otherwise form an acceptable basic-tier match. If this capacity absorption condition fails, priority separation alone does not rule out unmatched advanced nurses serving basic requests after exhausting acceptable advanced requests.

If no cross-tier priority is imposed by the fixed tiebreaker, replacing the weak inequality in Eq (6.3) with a strict inequality provides a tie-breaker-independent sufficient condition.

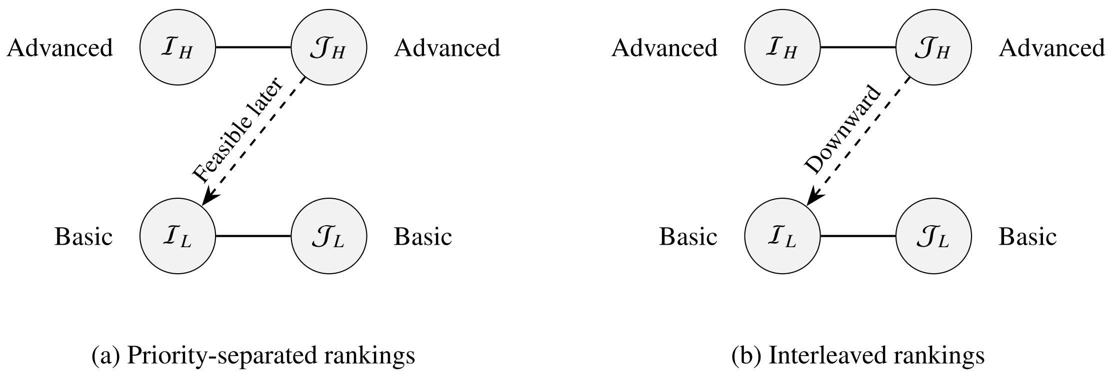

Figure 3. Tiered compensation can change the ordering of cross-tier alternatives. A dashed cross-tier edge remains clinically feasible in both panels; priority separation determines when it is considered, not whether it exists.

In the interleaved regime, a nearby basic request can outrank a distant advanced request, potentially displacing advanced demand. Proposition 3 deliberately does not claim monotonic changes in Q_H or Q_L: Preference changes can generate assignment cascades in general networks. The direction and magnitude of cannibalization are therefore evaluated numerically under stated market conditions.

6.4. *Two-dimensional equilibrium-constrained pricing*

Let k_H and k_L be platform costs by service tier. The pricing problem is

$$\max_{(p_H,p_L)\in\mathcal{P}_2} \quad \Pi(\boldsymbol{p}) = \sum_{\ell\in\{H,L\}} [(1-\eta_\ell)p_\ell - k_\ell] Q_\ell(\boldsymbol{p}, \mu_{\boldsymbol{p}}^N) \tag{6.4}$$

$$\text{s.t.} \quad \mu_{\boldsymbol{p}}^N = \Phi_N(\mathcal{I}_H \cup \mathcal{I}_L, \mathcal{J}_H \cup \mathcal{J}_L, \succ_{\mathcal{I}} (\boldsymbol{p}), \succ_{\mathcal{J}} (\boldsymbol{p})), \tag{6.5}$$

where $\mathcal{P}_2$ is a nonempty finite, institutionally admissible price menu grid. It may use tier-specific bounds, and increments and need not equal, or be contained in, the Cartesian square of the single-tier grid $\mathcal{P}_\Delta$. A full search over both prices is required to claim a two-dimensional optimum. Holding p_L fixed and varying $p_H - p_L$ is instead a price-spread sensitivity experiment. Section 7 reports these two exercises separately.

7. Numerical experiments

7.1. Scope and evidentiary status

We do not have access to transaction-level requests, posted fees, nurse availability, rejected offers, or realized assignments from a home nursing platform. Consequently, the numerical analysis is not an empirical calibration, structural estimation, empirical validation, or prediction of the profit-maximizing fee of a particular institution. Instead, we conduct externally anchored synthetic experiments. Publicly reported fee points, service radii, and the medical institution-affiliated workflow are used only to restrict the scale and institutional interpretation of the experiments. Behavioral and cost primitives that cannot be identified from those sources are explicitly treated as structural assumptions and subjected to sensitivity analysis. The numerical results therefore evaluate mechanism behavior and comparative robustness within the stated synthetic design; they should not be interpreted as estimated behavioral parameters, out-of-sample predictions, or actionable fee recommendations.

Every reported quantity Q is produced by the deferred acceptance algorithm on the mutually acceptable graph defined by Eqs (4.2)–(4.5). The numerical design therefore does not replace stable matching volume with the aggregate identity $Q = \min\{D, S\}$. Clinically incompatible, economically unacceptable, or locally bottlenecked pairs can remain unmatched even when aggregate demand and supply are both positive.

7.2. External anchors and parameter disclosure

Table 2. Baseline inputs and their evidentiary status.

Input	Baseline	Basis and status
Market geometry	10 km × 10 km; 10 km service radius	Stylized city scale with the within-city service radius anchored to [11]
Admissible fee grid	CNY 80–450 in CNY 10 increments	Brackets public fee points in [11] and [37]; externally anchored range, not an estimate
Nurse origins	Three stylized hospital centers; Gaussian displacement with 0.35 km standard deviation	Multicenter institutional structure; structural assumption compared with uniform origins
Patient valuation	Lognormal, median CNY 220, log-standard deviation 0.35	Assumed long-tailed heterogeneity; median varied from 180 to 260 and log-standard deviation from 0.20 to 0.50
Nurse attributes	Aggregate quality index $\sim$ Beta(4, 2); patient-specific weight with mean 50	Reduced-form representation of qualifications, experience, affiliation, and reputation; assumed
Patient spatial friction	Median $\gamma_i = 1.5$; $g(t) = t^{1.25}$	Distance importance externally motivated; magnitude and curvature assumed and stress-tested
Nurse opportunity cost	Lognormal, median CNY 60	Compensation matters in [3]; numerical level assumed and stress-tested over CNY 40–100
Nurse spatial friction	Median $\tau_j = 4$; $h(t) = t^{1.20}$	Commute effects externally motivated by [3, 4]; coefficient and curvature assumed and stress-tested
Payment parameters	Nurse share $\eta = 0.70$; platform cost $k = 20$ per order	Not publicly observed; assumptions disclosed separately from fee anchors
Compatibility	Pairwise probability 0.90 within the service radius	Reduced-form clinical, credential, and time window screening; assumed

The public price evidence provides a range rather than statistical estimates. In the Tianjin hospital case documented by [11], basic fees are CNY 80, 90, and 100 for regular services within 10 km; CNY

140, 160, and 180 for specialized services within 10 km; and CNY 300 and 450 for longer-distance services. The same study reports that service type and distance are important cost determinants and that 86.2% of patients were located in six areas around the physical hospital. A subsequent national policy report states that the separately listed home-service fee is concentrated at CNY 35–80 in primary institutions and CNY 100–200 in county-level and higher institutions, with the medical service item charged in addition [37]. We therefore search a deliberately wide CNY 80–450 grid. This range brackets public price points across service categories and distance bands; it does not imply that one standardized visit should cost the same across those categories.

Table 2 separates externally anchored inputs from assumed structural parameters. The public sources support the institutional workflow, selected fee points, the service radius scale, and the qualitative relevance of compensation, service duration, safety, and commute time. They do not identify the distributions of patient valuations, nurse opportunity costs, attribute weights, revenue shares, platform costs, or spatial friction coefficients used in the model. Those quantities are therefore disclosed as assumptions rather than calibrated or estimated parameters. The sensitivity analysis evaluates whether the reported mechanism patterns persist over the stated parameter ranges; it does not establish empirical external validity.

7.3. Experimental design and computational implementation

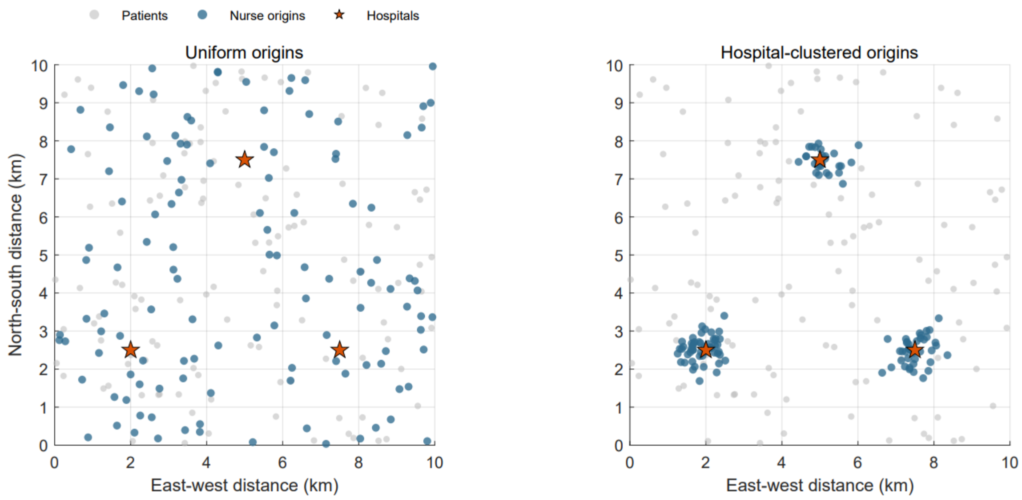

Figure 4. Uniform and hospital-clustered nurse origin designs. Patient locations remain citywide so that clustering changes the spatial coverage burden. Hospital coordinates are stylized rather than empirically geocoded.

We examine three market regimes. Supply surplus uses $(I, J) = (100, 140)$, balance uses $(120, 120)$, and demand surplus uses $(160, 100)$. Patients are distributed over the city. Patient locations are sampled independently from a uniform distribution over the 10 km × 10 km city in all experimental cells. This stylized benchmark is retained to isolate the effect of nurse origin clustering and is not interpreted as an empirically calibrated population density distribution. Nurse origins follow either a uniform benchmark or a distribution clustered around three stylized hospital centers. The centers represent a multi-institution configuration and are not claimed to be geocoded hospital locations. Figure 4 illustrates the two spatial designs using the same city boundary.

For every synthetic market and price, the code constructs patient and nurse preference lists over mutually acceptable pairs and runs nurse-proposing deferred acceptance. For replication r, let $\Pi_r(p)$, $Q_r(p)$, and $SW_r(p, \mu^N_{r,p})$ denote realized profit, completed volume, and welfare under the nurse-proposing rule. We use the smallest-maximizer convention and define

$$p^*_r = \min \arg \max_{p \in \mathcal{P}_\Delta} \Pi_r(p), \qquad p^Q_r = \min \arg \max_{p \in \mathcal{P}_\Delta} Q_r(p),$$

$W^N_r(p) = SW_r(p, \mu^N_{r,p})$, and $p^{W,N}_r = \min \arg \max_{p \in \mathcal{P}_\Delta} W^N_r(p)$. Thus, p^Q_r is the replication-level finite grid counterpart of the continuous volume benchmark p^V, and $p^{W,N}_r$ is the replication-specific nurse rule analog of $p^{SW}_{\Phi_N}$. In configuration-level tables and prose, the subscript r is suppressed, and the reported optimizer and welfare loss entries are Monte Carlo means of these replication-level quantities. The corresponding absolute and relative price-induced welfare losses are

$$L^{N,\mathrm{abs}}_r = W^N_r(p^{W,N}_r) - W^N_r(p^*_r), \tag{7.1}$$

$$L^{N,\mathrm{rel}}_r = \frac{W^N_r(p^{W,N}_r) - W^N_r(p^*_r)}{W^N_r(p^{W,N}_r)} \times 100\%, \qquad W^N_r(p^{W,N}_r) > 0. \tag{7.2}$$

These measures hold the clinical compatibility structure, stability requirement, and nurse-proposing selection rule fixed and isolate the welfare loss associated with the platform's posted price choice within that baseline mechanism. They are therefore conditional price-induced welfare losses. They are not the total welfare gap relative to a maximum weight clinically feasible assignment, nor do they measure the additional loss that may arise from selecting one stable matching rather than another. Each supply–demand–spatial configuration uses 100 independent replications. The sensitivity analysis uses 60 replications per parameter level and common random numbers across the levels of each factor. The tiered two-price grid is evaluated on 40 common synthetic markets. The separate price spread experiment holds $p_L = 160$, varies $p_H \in \{160, 180, \ldots, 440\}$, and uses 80 common markets. All reported uncertainty bands are normal-approximation 95% confidence intervals for Monte Carlo means. The master random seed is 20260808. In the tiered experiment, every candidate price pair is evaluated on the same set of synthetic markets.

The numerical experiments are implemented in MATLAB. Reported values are calculated from unrounded simulation outputs and are rounded only for presentation in the manuscript. Before completion, the implementation checks that the following hold: (i) The conditional finite-grid price-induced welfare loss is non-negative up to numerical tolerance; (ii) at the nurse-rule profit-maximizing fee in each of the 600 baseline markets, patient- and nurse-proposing deferred acceptance produce identical completed volume and platform profit; and (iii) no single-tier profit optimum occurs at either boundary of the admissible fee grid. The second check is conducted at the nurse-rule optimizer and is not a pointwise numerical comparison of the two profit curves over the full price grid.

7.4. Supply–demand regimes, spatial origins, and welfare loss

Table 3 reports all six baseline cells. Figure 5 plots the complete price curves for the hospital-clustered specification. Completed volume is hump-shaped because low fees can fail nurse individual rationality, and high fees can fail patient individual rationality; aggregate market counts alone do not determine realized stable volume.

Table 3. Pricing, matching, and welfare outcomes across market configurations.

Market	Nurse origins	p^*	p^Q	$p^{W,N}$	$Q(p^*)$	$\Pi(p^*)$	$L^{N,\text{abs}}$ (CNY);$L^{N,\text{rel}}$ (%)
Supply surplus	Uniform	218.9 (3.1)	118.9	119.6	73.93 (1.30)	3349.15 (31.15)	2700.84; 14.41 (0.80)
Balanced	Uniform	215.7 (2.7)	149.1	154.7	87.53 (1.50)	3888.65 (43.64)	2311.51; 10.96 (0.79)
Demand surplus	Uniform	234.0 (1.7)	178.2	225.8	95.57 (0.76)	4792.19 (44.16)	319.87; 1.47 (0.39)
Supply surplus	Clustered	215.7 (2.8)	131.9	133.4	73.96 (1.24)	3284.80 (37.36)	2300.84; 13.03 (0.76)
Balanced	Clustered	214.0 (2.8)	157.1	162.8	87.21 (1.52)	3826.32 (37.61)	1899.44; 9.53 (0.74)
Demand surplus	Clustered	230.9 (1.7)	187.0	222.4	95.41 (0.77)	4693.96 (36.79)	325.88; 1.56 (0.36)

*Notes: Monetary values are CNY. Entries are Monte Carlo means. Parentheses following p^*, $Q(p^*)$, $\Pi(p^*)$, and the relative welfare-loss percentage are 95% confidence interval half-widths. The welfare loss measures are conditional on nurse-proposing deferred acceptance and compare the profit-maximizing grid fee with the welfare-maximizing grid fee under the same selection rule; they are not total first best deadweight loss estimates.

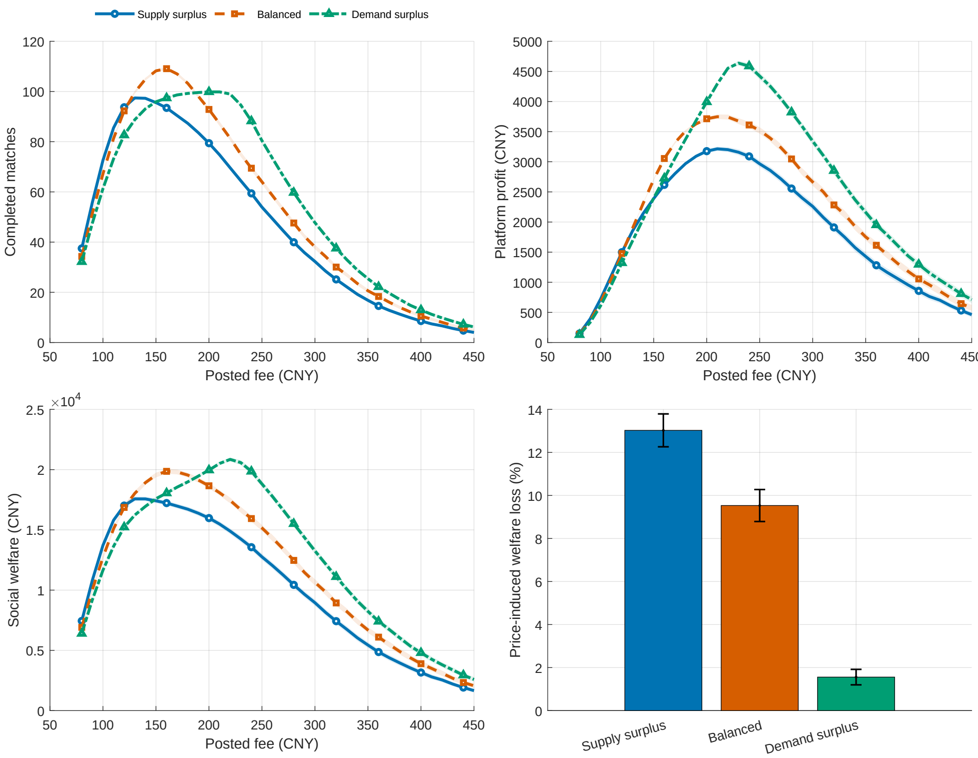

Figure 5. Price curves and nurse-rule-conditional price-induced welfare loss under hospital-clustered nurse origins. Shaded regions and error bars are 95% confidence intervals for Monte Carlo means.

Three patterns emerge within this design. First, the mean optimal fee lies between CNY 214.0 and 234.0, whereas the volume-maximizing fee changes much more strongly with relative scarcity. At the replication level, $p_r^* > p_r^Q$ in all 600 baseline markets. This finite-grid ordering is directionally consistent with the continuous fluid comparison $p^\Pi > p^V$ in Proposition 2, but the experiment does not separately estimate the local derivative in Equation (5.6) or verify the proposition's continuous single-peakedness condition; it is therefore not a direct numerical test of those sufficient conditions. Second, under the nurse-rule conditional benchmark, the mean absolute price-induced welfare loss ranges from CNY 319.87 to 2700.84, and the corresponding mean relative loss ranges from 1.47% to 14.41%. Across the 600 replications, $p_r^* \geq p_r^{W,N}$ always, and the inequality is strict in 85.5% of cases. These values quantify the welfare consequence of choosing the profit-maximizing posted fee rather than the welfare-maximizing grid fee while holding nurse-proposing deferred acceptance fixed. They do not represent a universal monopoly deadweight loss rate or the total gap relative to a first best clinically feasible assignment. Within the six synthetic configurations, the conditional loss is largest when supply is abundant and substantially smaller under demand surplus.

Third, replacing uniform nurse origins with hospital clustering raises mean matched travel from 1.02–1.16 km to 2.20–2.36 km because patients remain dispersed citywide, yet it changes the mean optimal fee by only 1.7–3.2 CNY within the corresponding supply–demand regimes. The profit-optimal fee is therefore comparatively robust to this spatial redesign, whereas travel burden and total welfare are not. The result supports reporting spatial service quality separately from the pricing objective.

7.5. Restricted numerical check of the stable selection rule

As a restricted numerical consistency check, we compute patient-proposing deferred acceptance at the nurse-rule profit-maximizing fee in each of the 600 baseline synthetic markets. At those prices, the maximum absolute difference in completed volume and platform profit is zero. This result is consistent with Corollary 1 but does not constitute a numerical comparison of the two rules at every price on the grid. Pointwise equality of completed volume and platform profit and hence, invariance of the profit-maximizing price set, follow from the theoretical rural hospitals argument under one-to-one matching, strict preferences, and margins that depend only on price and service type.

Assignments and welfare may nevertheless differ. Across the six baseline configurations, the mean patient-rule-minus-nurse-rule welfare difference at the nurse-rule optimizer ranges from −0.138 to 0.245 CNY, with a maximum absolute replication-level difference of 14.54 CNY. The maximum absolute travel distance difference is 0.015 km. These small numerical differences are specific to the present dense synthetic graphs and are not implied by Corollary 1. The present experiment therefore supports only a local consistency check at the nurse-rule optimizer; the general profit invariance conclusion remains a theoretical result conditional on the maintained assumptions.

7.6. Sensitivity to heterogeneous preferences and nonlinear spatial friction

Figure 6 varies five elements around the balanced, hospital-clustered baseline. Patient value medians are 180, 220, and 260; value log-standard deviations are 0.20, 0.35, and 0.50; nurse opportunity cost medians are 40, 60, and 100; nurse travel coefficients are 2.5, 4, and 6; and the low, baseline, and high distance curvature pairs (κ, ν) are $(1, 1)$, $(1.25, 1.20)$, and $(1.50, 1.40)$. The first curvature case reproduces linear distance friction, so this comparison directly addresses whether convex friction changes the main conclusions.

Valuation parameters are the most consequential within the tested ranges. Raising the valuation median from 180 to 260 increases the mean optimal fee from 186.0 to 244.7 CNY. Raising the valuation log-standard deviation from 0.20 to 0.50 increases the mean optimal fee from 210.8 to 229.2 CNY, reduces completed matches from 99.95 to 74.28, and raises mean conditional price-induced welfare loss from 6.78% to 12.62%. Thus, replacing heterogeneous values with a representative patient would materially understate tail-driven price extraction within the stated synthetic design.

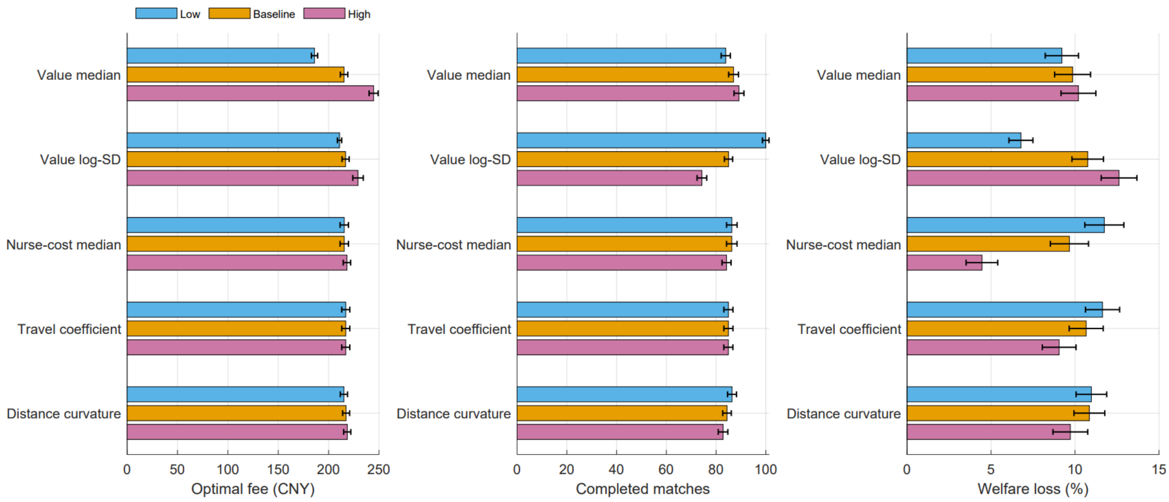

Figure 6. Sensitivity of the profit-optimal fee, completed matches, and nurse-rule-conditional price-induced welfare loss. Each factor uses common random numbers across its low, baseline, and high levels; error bars are 95% confidence intervals.

The optimal fee is more stable under the supply cost and spatial stress tests. Raising median nurse opportunity cost from 40 to 100 CNY changes the mean optimal fee from 215.5 to 218.2 CNY and completed volume from 86.32 to 84.20; it lowers the relative conditional price-induced welfare loss because the welfare benchmark itself loses feasible low-cost edges. Increasing the nurse travel coefficient from 2.5 to 6 leaves the mean grid optimizer at CNY 217.0 and completed volume virtually unchanged at 84.95 versus 84.93 in the common-random-number comparison, while reducing welfare at any given matching. Moving from linear friction, $(\kappa, \nu) = (1, 1)$, to the high-curvature specification, $(1.50, 1.40)$, raises the mean optimal fee from CNY 215.2 to 218.5 and reduces the completed volume from 86.40 to 82.80. These are robustness findings for the stated range, not global comparative static claims: Proposition 1 guarantees edge-set contraction, not monotonic movement of p^*. Moreover, unchanged completed volume is not evidence that the feasible edge set is unchanged because removed edges need not belong to the selected stable matching; the present sensitivity output evaluates matching outcomes rather than directly tabulating $|\mathcal{E}(p)|$. The present spatial robustness analysis compares uniform and three-center clustered origins but does not vary the number of centers or the within-center dispersion; these dimensions require geocoded institutional data and remain outside the current synthetic design.

7.7. Two-dimensional tiered pricing and downward substitution

The tiered experiment contains 60 advanced and 100 basic requests, 60 advanced and 70 basic nurses, hospital-clustered origins, and the clinical restriction that basic nurses cannot serve advanced requests. We search $p_L \in \{80, 100, \ldots, 300\}$ and $p_H \in \{140, 160, \ldots, 460\}$ subject to $p_H \geq p_L$. The full two-dimensional search over Monte Carlo mean profit selects $(p_H, p_L) = (320, 200)$ CNY. At this grid point, mean profit is CNY 6087.89 ± 66.68, mean advanced and basic completed volumes are

43.65 ± 0.88 and 74.28 ± 0.97, and mean downward substitutions are 15.28 ± 0.82, where the plus-minus values are 95% confidence interval half-widths.

The right panel of Figure 7 shows why a price gap experiment is not a substitute for the two-dimensional search. With $p_L = 160$, mean downward substitution first falls from 38.56 at $\Delta w = 6.4$ to 5.54 at $\Delta w = 78.4$, but then rises to 37.91 at $\Delta w = 208$. The initial decline reflects advanced nurses' stronger priority for advanced requests. At very high p_H, however, patient individual rationality removes advanced requests, leaving advanced capacity to spill into basic service. Hence, a larger compensation premium is not a monotone "geographic firewall". One sufficient safeguard is to combine priority separation with a high-tier-only submarket that satisfies the absorption condition in Proposition 3. The experiment records realized assignments but does not tabulate the realization-specific threshold in Eq (6.3) or the number of advanced nurses absorbed by the high-tier-only submarket. The nonmonotone curve is therefore consistent with the proposition and illustrates why its capacity condition matters, but it is not a direct numerical verification of the sufficient condition.

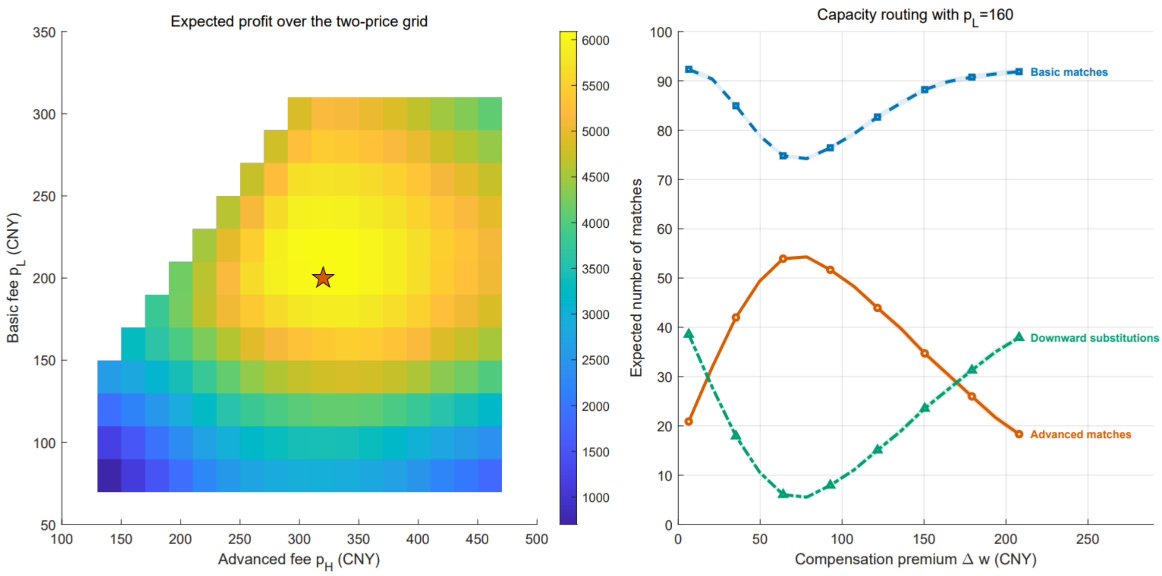

Figure 7. Two-dimensional tiered-price search and price spread sensitivity. The star marks the expected-profit maximizer. The right panel holds $p_L = 160$ and measures the advanced service compensation premium as $\Delta w = 0.72p_H - 0.68p_L$.

8. Conclusion

This study develops an institutionally and mathematically consistent framework for price-induced stable matching in platform-mediated home healthcare. A common service fee changes participation and the set of mutually acceptable edges but does not reorder within-tier preferences, whereas tier-specific nurse compensation can reorder cross-tier preferences and generate downward substitution. The operational model admits an optimal fee on any nonempty finite admissible price grid under the stated weak participation and deterministic tiebreaking conventions. Platform profit and the set of profit-maximizing prices are invariant across stable selection rules when the platform margin depends only on price and service type, although assignments, surplus distribution, travel, and welfare may differ. The analysis also shows that priority separation across skill tiers does not by itself guarantee zero downward substitution; under the maintained nurse-proposing rule, the stated capacity absorption condition provides a sufficient additional guarantee.

The externally anchored synthetic experiments quantify these mechanisms without claiming empirical calibration or validation. Across the six supply–demand and spatial configurations, the mean profit-optimal fee ranges from CNY 214.0 to CNY 234.0. Conditional on the baseline nurse-proposing stable selection rule, the mean price-induced welfare loss relative to the welfare-maximizing grid fee ranges from 1.47% to 14.41%. These percentages describe pricing distortion within the maintained mechanism and are not estimates of total first best deadweight loss for an actual platform. Hospital-clustered nurse origins substantially increase matched travel but change the profit-optimal fee only modestly. Patient-valuation dispersion has a stronger effect on the optimal fee, completed volume, and conditional welfare loss than the tested nurse-cost and spatial friction ranges. The tiered experiment further illustrates that an excessively high advanced service fee can recreate downward substitution by suppressing advanced patient participation, even when the resulting compensation premium strengthens advanced nurses' preference for advanced requests.

These findings suggest three managerial implications. First, platforms should evaluate pricing jointly with the stable assignment it induces rather than infer completed volume from aggregate supply and demand alone. Second, geographic service quality and travel burden should be reported alongside profit because similar optimal fees can conceal materially different spatial outcomes. Third, tiered compensation should be coordinated with advanced demand and available capacity; increasing the fee or compensation spread alone does not provide a monotone safeguard against downward substitution.

Several limitations define the scope of these conclusions and motivate targeted next steps. Public information constrains the fee range and service radius but does not identify patient valuations, nurse opportunity costs, revenue shares, or acceptance behavior. Patient locations and hospital centers remain stylized, and the numerical model represents a single service block rather than repeated participation or multivisit routing. Consequently, the reported price levels should be interpreted as mechanism-based numerical stress tests rather than actionable recommendations for a particular platform. Future empirical work should assemble a deidentified panel containing service types, coarse origin cells, posted fees, available nurses, displayed attributes, accept/reject decisions, assignments, travel times, durations, cancellations, and completion outcomes. Such data would permit estimation of the behavioral and cost primitives. Institutions, regions, or time periods should then be reserved as holdout samples for out-of-sample comparisons of predicted and realized participation, assignments, travel, cancellations, and completion outcomes. Subsequent extensions could replace the stylized spatial process with institution and population density data, endogenize nurse entry, and retention and patient return, and integrate PISM with multivisit home healthcare routing and scheduling.

Author contributions

Xiaowei Lin: Conceptualization, methodology, Software, Formal analysis, Writing-original draft preparation. Yun Wei: Conceptualization, validation, resources, writing-review & editing. All authors have read and agreed to the published version of the manuscript.

Use of Generative-AI tools declaration

During the preparation of this work, the authors used Google Gemini and ChatGPT to assist with LaTeX formatting and to debug the MATLAB code for numerical simulations. The authors thoroughly reviewed, tested, and validated all generated code/outputs and take full responsibility for the accuracy and integrity of the final manuscript.

Acknowledgments

This work was partially funded by the Humanities and Social Science Foundation of Ministry of Education of China (Grant No. 22YJCZH101), Start-Up Funds of Nanjing Vocational University of Industry Technology (Grant No. YK21-12-04).

Conflict of interest

The authors declare no conflict of interest.

References

1. National Health Commission of China, *Notice on launching the pilot program of "Internet Plus Nursing Services"*, 2019. Available from: https://www.nhc.gov.cn/yzygj/c100068/201902/5b2c18d54d0c487db84562fe2c780114.shtml.
2. National Health Commission of China, *Notice on further advancing the pilot program of "Internet Plus Nursing Services"*, 2020. Available from: https://www.nhc.gov.cn/yzygj/c100068/202012/f858a52b12a246649d53531ddc120eab.shtml.
3. Y. He, G. Feng, C. Wang, D. Yang, L. Hu, W.-K. Ming, et al., Nurses' job preferences on the Internet Plus Nursing Service program: A discrete choice experiment, *BMC Nurs.,* **23** (2024), 120. https://doi.org/10.1186/s12912-023-01692-0
4. J. Yang, B. Ma, S. Chen, Y. Huang, Y. Wang, Y. Chen, et al., Nurses' preferences for working in Uber-style "Internet Plus" nursing services: A discrete choice experiment, *Int. J. Nurs. Stud.,* **161** (2025), 104920. https://doi.org/10.1016/j.ijnurstu.2024.104920
5. A. M. Fathollahi-Fard, M. Hajiaghaei-Keshteli, R. Tavakkoli-Moghaddam, A bi-objective green home health care routing problem, *J. Clean. Prod.,* **200** (2018), 423–443. https://doi.org/10.1016/j.jclepro.2018.07.258
6. C. Fikar, P. Hirsch, Home health care routing and scheduling: A review, *Comput. Oper. Res.,* **77** (2017), 86–95. https://doi.org/10.1016/j.cor.2016.07.019
7. M. Reula, C. Parreño-Torres, C. Lamas-Fernandez, A. Martinez-Sykora, A flexible mathematical model for home health care problems, *Eur. J. Oper. Res.,* **327** (2025), 791–807. https://doi.org/10.1016/j.ejor.2025.05.055
8. S. Atta, V. Basto-Fernandes, M. Emmerich, A concise review of the home health care routing and scheduling problem, *Oper. Res. Perspect.,* **15** (2025), 100347. https://doi.org/10.1016/j.orp.2025.100347

9. D. Khorasanian, J. Patrick, A. Sauré, Dynamic home care routing and scheduling with uncertain number of visits per referral, *Transp. Sci.,* **58** (2024), 841–859. https://doi.org/10.1287/trsc.2023.0120
10. M. Lin, L. Ma, C. Ying, Matching daily home health-care demands with supply in service-sharing platforms, *Transp. Res. Part E Logist. Transp. Rev.,* **145** (2021), 102177. https://doi.org/10.1016/j.tre.2020.102177
11. Y. Wang, Y. Liu, Z. Jin, C. Jin, F. Hu, T. Yu, An Internet hospital plus home nursing model for chronic disease patients: Mixed-methods study in Tianjin, China, *JMIR Nurs.,* **8** (2025), e76761. https://doi.org/10.2196/76761
12. N. Chen, D. Bai, N. Lv, Towards an integrated online–offline healthcare system: Exploring Chinese patients' preferences for outpatient follow-up visits using a discrete choice experiment, *Systems,* **12** (2024), 75. https://doi.org/10.3390/systems12030075
13. N. Chen, D. Bai, J. Ning, A determination of patient preferences for China online outpatient follow-up clinics by using discrete choice experiment: An exploratory study, *Front. Public Health,* **13** (2025), 1508369. https://doi.org/10.3389/fpubh.2025.1508369
14. M. Armstrong, Competition in two-sided markets, *RAND J. Econ.,* **37** (2006), 668–691. https://doi.org/10.1111/j.1756-2171.2006.tb00037.x
15. J. C. Rochet, J. Tirole, Platform competition in two-sided markets, *J. Eur. Econ. Assoc.,* **1** (2003), 990–1029. https://doi.org/10.1162/154247603322493212
16. S. R. Balseiro, D. B. Brown, C. Chen, Dynamic pricing of relocating resources in large networks, *Manag. Sci.,* **67** (2020), 4075–4094. https://doi.org/10.1287/mnsc.2020.3735
17. O. Besbes, F. Castro, I. Lobel, Surge pricing and its spatial supply response, *Manag. Sci.,* **67** (2020), 1350–1367. https://doi.org/10.1287/mnsc.2020.3622
18. K. Bimpikis, O. Candogan, D. Saban, Spatial pricing in ride-sharing networks, *Oper. Res.,* **67** (2019), 744–769. https://doi.org/10.1287/opre.2018.1800
19. G. P. Cachon, K. M. Daniels, R. Lobel, The role of surge pricing on a service platform with self-scheduling capacity, *Manuf. Serv. Oper. Manag.,* **19** (2017), 368–384. https://doi.org/10.1287/msom.2017.0618
20. J. C. Castillo, D. Knoepfle, E. G. Weyl, Matching and pricing in ride hailing: Wild goose chases and how to solve them, *Manag. Sci.,* **71** (2024), 4377–4395. https://doi.org/10.1287/mnsc.2022.00096
21. Q. Chen, Y. Lei, S. Jasin, Real-time spatial–intertemporal pricing and relocation in a ride-hailing network: Near-optimal policies and the value of dynamic pricing, *Oper. Res.,* **72** (2023), 2097–2118. https://doi.org/10.1287/opre.2022.2425
22. H. Guda, U. Subramanian, Your Uber is arriving: Managing on-demand workers through surge pricing, forecast communication, and worker incentives, *Manag. Sci.,* **65** (2019), 1995–2014. https://doi.org/10.1287/mnsc.2018.3050
23. T. A. Taylor, On-demand service platforms, *Manuf. Serv. Oper. Manag.,* **20** (2018), 704–720. https://doi.org/10.1287/msom.2017.0678
24. C. Yan, H. Zhu, N. Korolko, D. Woodard, Dynamic pricing and matching in ride-hailing platforms, *Naval Res. Logist.,* **67** (2020), 705–724. https://doi.org/10.1002/nav.21872

25. D. Gale, L. S. Shapley, College admissions and the stability of marriage, *Amer. Math. Monthly,* **69** (1962), 9–15. https://doi.org/10.1080/00029890.1962.11989827
26. A. E. Roth, The evolution of the labor market for medical interns and residents: A case study in game theory, *J. Political Econ.,* **92** (1984), 991–1016. https://doi.org/10.1086/261272
27. A. E. Roth, On the allocation of residents to rural hospitals: A general property of two-sided matching markets, *Econometrica,* **54** (1986), 425–427. https://doi.org/10.2307/1913160
28. J. W. Hatfield, P. R. Milgrom, Matching with contracts, *Amer. Econ. Rev.,* **95** (2005), 913–935. https://doi.org/10.1257/0002828054825466
29. A. S. Kelso, V. P. Crawford, Job matching, coalition formation, and gross substitutes, *Econometrica,* **50** (1982), 1483–1504. https://doi.org/10.2307/1913392
30. J. H. Blanchet, M. I. Reiman, V. Shah, L. M. Wein, L. Wu, Asymptotically optimal control of a centralized dynamic matching market with general utilities, *Oper. Res.,* **70** (2022), 3355–3370. https://doi.org/10.1287/opre.2021.2186
31. R. Johari, V. Kamble, Y. Kanoria, Matching while learning, *Oper. Res.,* **69** (2021), 655–681. https://doi.org/10.1287/opre.2020.2013
32. Y. Kanoria, D. Saban, Facilitating the search for partners on matching platforms, *Manag. Sci.,* **67** (2021), 5990–6029. https://doi.org/10.1287/mnsc.2020.3794
33. E. Özkan, A. R. Ward, Dynamic matching for real-time ride sharing, *Stoch. Syst.,* **10** (2020), 29–70. https://doi.org/10.1287/stsy.2019.0037
34. S. M. Varma, P. Bumpensanti, S. T. Maguluri, H. Wang, Dynamic pricing and matching for two-sided queues, *Oper. Res.,* **71** (2022), 83–100. https://doi.org/10.1287/opre.2021.2233
35. A. Bassamboo, J. M. Harrison, A. Zeevi, Design and control of a large call center: Asymptotic analysis of an LP-based method, *Oper. Res.,* **54** (2006), 419–435. https://doi.org/10.1287/opre.1060.0285
36. I. Gurvich, M. Armony, C. Maglaras, Cross-selling in a call center with a heterogeneous customer population, *Oper. Res.,* **57** (2009), 299–313. https://doi.org/10.1287/opre.1080.0568
37. National Healthcare Security Administration of China, *Implementation of home medical service pricing policies: New development in inclusive and convenient health care*, 2026. Available from: https://www.nhsa.gov.cn/art/2026/4/24/art_14_20316.html.

AIMS Press